DOI : https://doi.org/10.56452/7-8-41

ISSN: 0974-5823 Vol. 7 No. 8 August, 2022

International Journal of Mechanical Engineering

Active Power And Harmonic Current Control Loop For Single Stage Solar Inverter Using Hybrid Filters With Power Quality Reinforcement: A HUA-BCMO Approach

Palarapu Sravan Kumar *

*Electrical Engineering Department, University College of Engineering,Osmania University, Hyderabad, India-500007, sravaneeeastra@gmail.com,

Dr. B Mangu

**Electrical Engineering Department, University College of Engineering,Osmania University, Hyderabad, India-500007, bmanguou@gmail.com

***Corresponding Author;**Palarapu Sravan Kumar

*Research Scholar, Electrical Engineering Department, Osmania University, Hyderabad, India-500007, Tel: +91 9666645035, sravaneeeastra@gmail.com

Abstract

Single stage solar inverter using hybrid filters with power quality reinforcement using shunt active hybrid filter (SHF) is proposed in the manuscript. The aimed hybrid method are the integration of Human urbanization algorithm (HUA) and Balancing Composite Motion Optimization (BCMO), hence it is named HUA-BCMO approach. In the proposed work, there are two control loops are considered, they are, active power control (APC) and harmonic current control (HCC) loop. Power from the solar panel to the grid is supplied by APC loop that is carried out by HUA control approach. Compensation of harmonic current produced by nonlinear loads is performed by BCMO approach using harmonic current control loop. BCMO approach is very effectively compensates the harmonic currents from source. These loops are utilized to the PI controllers for control the current and power. The harmonics are compensated by voltage-mode control and control the power converter. Compensation voltage is produced via the power converter that is converted into compensating current to facilitate filter harmonic currents produced in non-linear loads. Here, the feedback is considered as harmonic current of the grid and reference as grid harmonic currents under the state of ideal filter. The aimed approach is implemented in MATLAB/Simulink platform, and then the efficiency is compared with various existing approaches.

Keywords: *Power quality, Solar Panel, Harmonic current, Non-linear load, Active power control, PI controller.*

1. Introduction

The global warming and demanding loads are environmentally friendly energy, which is the solution of next generation. Renewable-based technology is required to gradually provide sustainable and pollution-free technology [1]. Some of the advantages of Renewable-based technology are possibility of clean, lesser effects in the environment and more energy storage resources such as sun and wind. Here the combination of both renewable energy sources (RESs) and energy storage systems are the essential task [2]. Nowadays, environmental benefits and penetration of hybrid renewable energy sources (HRESs) have developed speedily. The idea of distributed power generation, known as microgrid (MG), progresses, the combination of HRES with the battery storage system can prevent problems at a time when the load is meet the power requirement

[3-5]. Additionally, backup energy source is a battery storage system that provides the power needed to load. A combination of a pair of RES at all levels cannot meet all load requirements, so a battery storage system is necessary to meet the requirement of energy [6-8].

A solar photovoltaic is a major factor of renewable power generation that are connected to the grid through the high power electronic inverters. Because a power conversion capacity module is relatively low, using high capacity power conditioners can reduce the overall system cost [9-10]. Commonly, the high grid voltage is greater than the dc connection voltage of photovoltaic source based on topology output voltage is varied then the operation consist of two levels. In the first level, the photovoltaic voltage is boosted via dc to dc converter and the next level can converts into AC voltages [11-12]. However, the components usage and levels are increased, but the efficiency is decreased. So the topology based on single-stage inverter is gaining more interest. The PV module, the inverter is essential in series connection; due to this the voltage of PV is maintained high compared to input voltage. When individual panels are operated under different conditions, these long panels can cause many problems such as large size and poor performance [13-14].

The single stage solar inverter depend on current source inverter (CSI) is need bulky inductor in DC side, so the loss is high [15-16]. Also, in CSI filtering it becomes difficult to change the ripple on the grid side. In the last decades, power electronics based on utility systems in factories provides rapid increase in loads. The magnitude of the harmonic distortion is because of the supply current in the electrical system is raised by the multiplication of non-linear loads [17-18]. To reduce the harmonics including reactive power compensation, Hybrid active filters are developed to incorporate the passive filter in series together with active filter. High resistance provided by the passive filter under fundamental frequency so hybrid filter is not required. Accordingly, for harmonic compensation, the less dc link voltage is needed. Yet, the harmonic compensation purpose is, to less the dc need link voltage which also utilized in single stage solar inverters on power quality improvement [19-20].

This manuscript proposes a hybrid method of single stage solar inverter with power quality reinforcement using shunt active hybrid filter. The suggested hybrid method are the combined execution of Human urbanization Algorithm- Balancing Composite Motion Optimization, hence it is named HUA-BCMO approach. Remainder of this suggestions is structured as: Section two presents the recent research work. Section three illustrates the configuration of single stage solar inverter with control of suggested approach**.** Section four explains the issues which affect the quality of power. Section five describes about the proposed approach based power quality improvement. Section six evidence the simulating result and discussion. Section seven presents conclusion.

2. Recent Research Works: A Brief Review

Various researchers were previously presented in the paper based upon power quality enhancement with hybrid filters in renewable sources utilizing certain strategies with aspects. Several related works were shown here,
S. Echalih *et al.* [21] introduced a fuzzy logic controller method for controlling of shunt active power filter (SAPF) with nonlinear loads. Dual Buck Half Bridge converter (DBHB) based SAPF was utilized for the removal of shoot-through problem. The major objective of the suggested approach was design of controller which provides harmonic component assessment. By utilizing the introduced approach, three ways were utilized to achieve the objective such as, harmonic components determination in indirect and simple way, through the nonlinear load harmonic as well as reactive currents were produced which was compensated and ensure acceptable power factor correction on the grid side, DBHB converter, dc capacitor voltage was regulated. The introduced approach was utilized into two loops such as inner loop, outer loop. The control law was designed by hybrid automaton of DBHB-SAPF which was performed in the inner loop. Unity power factor were guaranteed by the inner loop. The control of dc voltage converter to the optimum value was guaranteed by the fuzzy logic controller which was operated in the outer loop. M. Badoni *et al.* [22] have presented the fractional order notch filter (FONF) to increase the quality of power to grid-connected PV system. From the distorted load currents, the basic active ingredients was determined by the introduced filter, therefore, the PV system was utilized the gating pulses for operating voltage source converter (VSC). Harmonics distortion, reactive power burden, unbalancing of connected load were considered as the issues of quality of power. Babu *et al.* [23] have suggested fuzzy logic PID-multi-complex coefficient filter-multi- second-order generalized integrator-frequency-locked loop (FLPID-MCCF-MSOGI-FLL) based SHF as an improvement of power quality of grid connected PV system. Through the extraction of basic constituent through the nonlinear load

currents, the harmonic currents were mitigated by the MSOGI-FLL reference current generation approach. The voltage harmonics were eliminated by MCCF which separates the basic constituent from the decayed grid voltages. The steady power among dc and ac sides was maintained through the FLPID approach that was obtained by controlling the dc connection voltage stable under transient stages. The particle swarm optimization based perturbs was used to obtain the maximal power from the photovoltaic system.

A. K. Mishra *et al.* [24] have suggested the hybrid Particle Swarm Optimization-Grey Wolf Optimization (PSO-GWO) to improve the power quality of PV system. Where, HSAPF was utilized. Under the balanced and unbalanced loading conditions, the FIPID controller was utilized to compensate the reactive power and harmonics. Through PSO-GWO approach, the parameters of FOPID were tuned which eliminate the harmonics. I.D. Melo *et al.* [25] have postulated genetic algorithm for assigning and sizing of filters in power distribution systems. The intention of the suggested method was lessening of total harmonic distortion. To utilize the inequality constraints the Upper and lower bounds are used for power factor correction, tuned frequency, voltage imbalance factor, voltage magnitudes, harmonic distortion were. The filter location, topology of filter, parameters were determined by the introduced approach for solve the optimization problem. G. Goswami and P. K. Goswami [26] have developed an adaptive neural fuzzy interface system (ANFIS) supervised PID controlled shunt active power filter to reduce the harmonics of the system. ANFIS was developed the reference current signal and control switching which provides the optimum PID action in conventional HSAPF. The feasibility of the system was monitored under the transient and steady-state condition. S. K. Prince *et al.* [27] have presented the dual extended Kalman filter (DEKF) control approach to improve the performance of shunt active power filter (SAPF). Grid power demand was reduced by supply of needed load power form the PV. The maximum power was extracted from PV using single sensor-based control. PSO was utilized for tuning the parameter of the SAPF. The reference signal was generated by determination of state as well as parameter of nonlinear system using DEKF.

2.1. Background of the Research Work

The research work review shows the power quality improvements in renewable system with hybrid filters is the most contributing factor. In the power system, the power quality plays significant role. The major renewable energy source among all renewable sources is solar photovoltaic because of its benefits like less carbon emission, abundant availability, and less environment pollution. But, power quality is affected by the interconnection of solar PV to grid. Due to uncertainty and low reliability, the PV system has many problems such as feeder overloading, harmonic distortion, large installation cost, less efficiency. Because of the changes in solar radiation based on the intermittent in nature are leads to voltage fluctuation and flicker. Inverters is an important role in the grid connected solar photovoltaic system, to maintain the quality of power. However, because of the non-linear loads in the system causes harmonics at DC to AC power conversion process of inverters. Due to this harmonics, heating effect, malfunction and permanent damage to electrical equipment was occurred. At first, passive filters are utilized to reduce the harmonics but it has some drawbacks like fixed compensation, large size with resonance in the distributed system. Then active filters were used to reduce the harmonics for various types of nonlinear loads. Though, the scaling of active filter is sometimes very close to load which provide cost problem. Due to the consideration of rating of AF and cost, its usage is limited. A series of hybrid filters is introduced to solve the cost problem to compensate the nonlinear loads. These hybrid filters (HFs) are used for compensate the different category of nonlinear loads. Hence, it was deemed to provide the hybrid filter with optimal techniques for handling the power community with power quality issues in a renewable system. These drawbacks have inspired to do this research work.

3. Configuration of Single Stage Solar Inverter with Control of Proposed Approach

Fig 1 portrays the configuration of single stage solar inverter. On observing this Figure, passive filter, active filter, and 3 phase full bridge VSI, PV module, non linear load are delineated. The passive filter is connected in series with an active filter with VSI and PV module. VSI is associated with DC bus. The seventh harmonic frequency [28] is used to decrease the passive filter measurement. Reactive power was supplied by the capacitor which uses to level delay load. Compared with conventional active filter, hybrid active filter is needed to small dc connection voltage rating due to series capacitance of LC filter used bulk of fundamental voltage. This is favored for single stage solar inverters as hybrid active filter needed lesser dc connection voltage likened with active filter. Less switching ripple, minimized installation space and power quality improvement are the

DOI : https://doi.org/10.56452/7-8-41

advantages of the proposed approach. In addition, the functioning efficiency of the proposed inverter are high when compared with active filter based solar inverter.

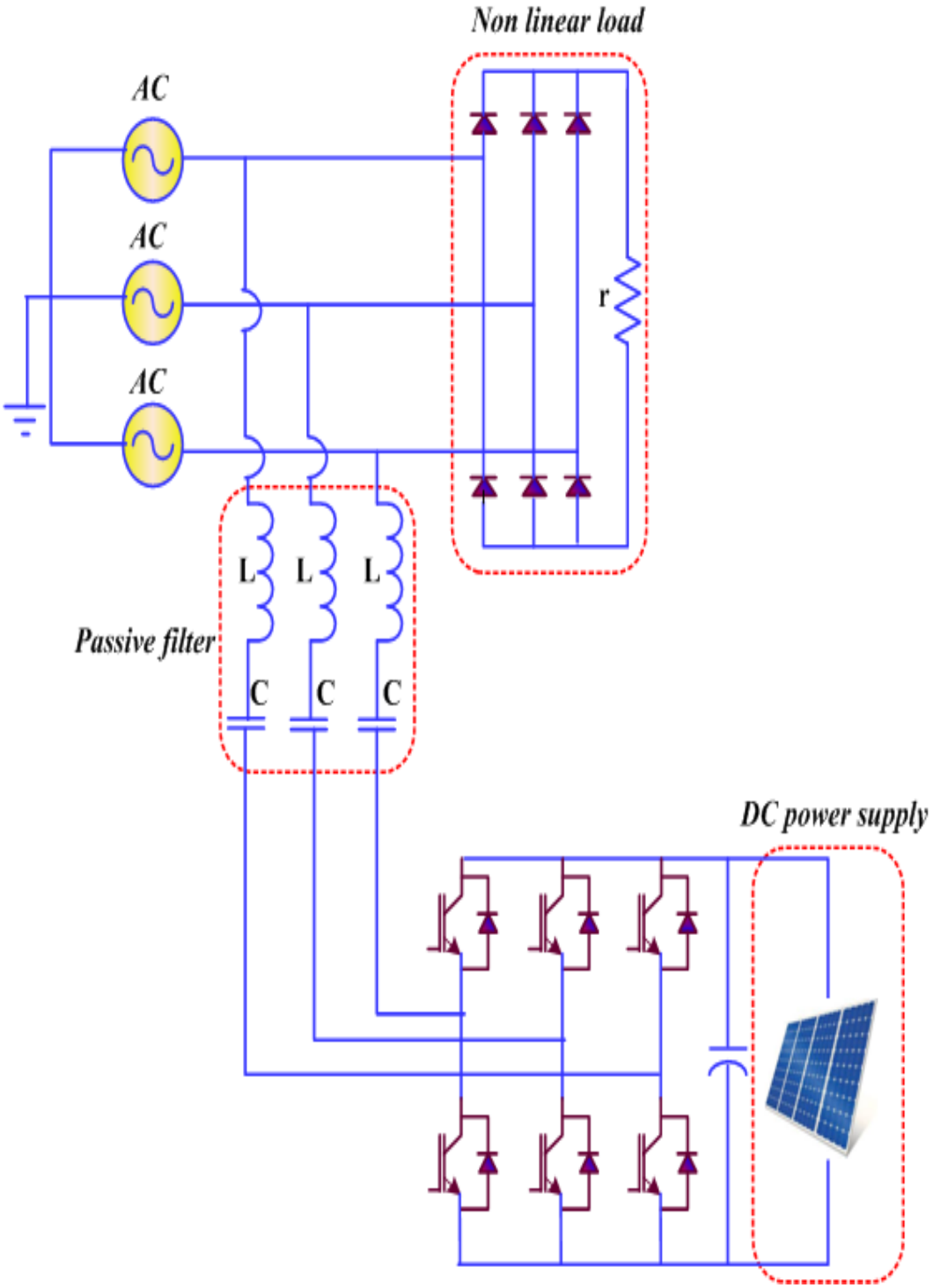

Fig 1: Configuration of single stage solar inverter

Figure 2 depicts the Control structure of the single-stage solar inverter with proposed approach. The proposed system is incorporated with APC and HCC. The active power control loop is performed in HUA approach. By utilizing the dq transform , the active power is adjusted.

DOI : https://doi.org/10.56452/7-8-41

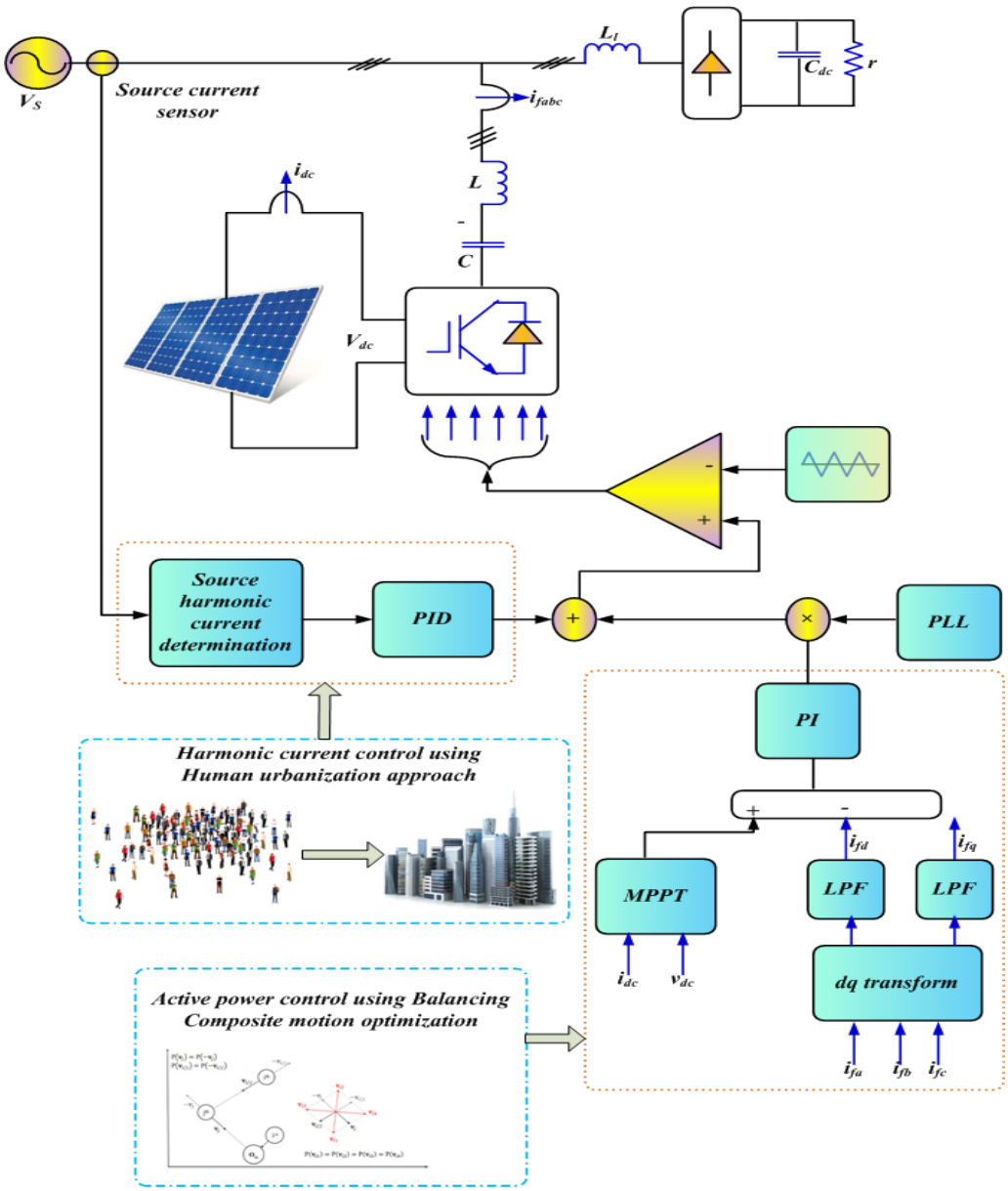

Fig 2: Control structure of the single-stage solar inverter with proposed approach

Through the active power control the power is injected from PV module to grid. The harmonic current control loop is performed as load side. For the harmonic current control, BCMO approach was utilized helpfully for compensating the harmonic currents from source.

3.1. Modelling of PV

In the Solar PV, the energy is generated depend on the weather condition, air temperature and the radiation of solar. The PV module outcome is defined as,

$$P_T^{PV} = P_{PV}^R \times r^D \times \left(\frac{G}{G_{STC}}\right) \times \left(1 + \alpha^P \left(T^c - T^{STC}\right)\right) \quad (1)$$

Here, Output power for solar cell is specified as P_T^{PV}, rated power for solar cell is indicated as P_{PV}^R, module operating factor is indicated as r^D, solar radiation is indicated as G, solar radiation as standard test conditions, [W/m^2] is indicated as G_{STC}, temperature coefficient is indicated as α^P ,cell temperature is indicated as T^c ,cell temperature of the solar panel at standard test condition is indicated as T^{STC}. The temperature of cell is expressed as,

DOI : https://doi.org/10.56452/7-8-41

$$T^{c} = T^{A} + \left(T^{c,noct} - T^{a,noct}\right)\left(\frac{G^{T}}{G^{T,noct}}\right) \times \left(1 - \frac{\eta_{PV}^{MPP}}{0.9}\right) \quad (2)$$

Here, ambient temperature is indicated as T^{a}, ambient temperature at which normal operating cell temperature (NOCT) condition is specified as $T^{a,noct}$,nominal operating PV cell temperature is specified as $T^{c,noct}$,Solar radiation on PV array is specified as G^{T}, Solar radiation at which NOCT [29] condition is specified as $G^{T,noct}$, efficiency of PV array at MPP is specified as η_{PV}^{MPP}.

3.2. DC Link Capacitor

Equation for the DC link capacitor was determined by,

$$C_{dc} = \frac{P_{dc} / V_{dc}}{2\omega V_{dcrip}} \quad (3)$$

Here, P_{dc} specifies dc connection power, V_{dc} specifies dc connection voltage, ω denotes angular frequency.

3.3. Phase Lock Loop (PLL)

The linear feedback control system is the PLL [30-31] which is utilized to produce the output signal which as the equal frequency as well as phase like the input reference signal. It is used to reduce the noise of the system.

3.4. Control of Active Power

When the filter voltage is zero, then the filter current supplies the voltage to grid [32-33]. The relation among the filter current and the supply voltage is described as,

$$i_{fq} = \frac{\vec{v}_S}{x_C} \quad (4)$$

Here, filter current is denoted as i_{fq}, supply voltage is denoted as v_S. The total voltage is the difference of vector sum of supply voltage and filter voltage which is described as,

$$\vec{v}_{Tot} = \vec{v}_S - \vec{v}_f = v_S + jv_f \quad (5)$$

If the currrent is flow through the filter then the filter current is described as,

$$i_f = \frac{j\vec{v}_{Tot}}{x_C} = j\left(\frac{v_S + jv_f}{x_C}\right) = j\frac{v_S}{x_C} - \frac{v_f}{x_C} = i_{fd} + ji_{fq} \quad (6)$$

Here, real components of filter current is $i_{fd} = -\frac{v_f}{x_C}$ and the reactive component of the filter is $i_{fq} = -\frac{v_S}{x_C}$.

The source voltage is lagging at the active component and straightforwardly related to inverter voltage v_f, the reactive component is directly proportional to the source voltage. Transformation of three phase currents to dq current is performed by the park transformation. In this d axis current, the active current is managed for creating q-axis voltage that are proportional to propositional integral Controller outcome. The unit vector is multiplied which lag the source voltage obtained from PLL. Due to the slow response of the PV module, PI controller is designed with 20 Hz bandwidth.

3.4.1. Mathematical Model of the Hybrid Active Filter in Active Current Control Loop

Fig 3 illustrates the block diagram of closed loop control system. The measurement model of hybrid active filter [34] was described as,

DOI : https://doi.org/10.56452/7-8-41

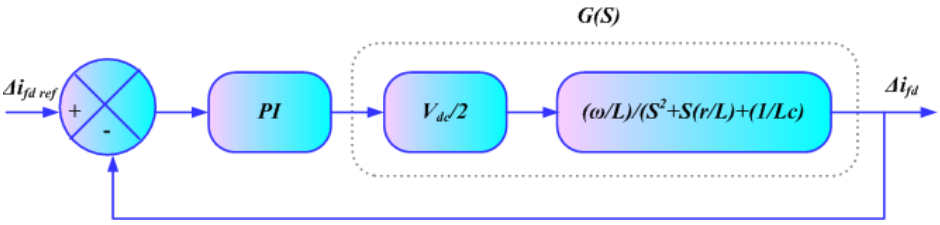

Fig 3: Block diagram of closed loop control

$$[v_S]_{ABC} = [i_f]_{ABC} * r + \frac{d[i_f]_{ABC}}{dt} * L + \frac{1}{c}\int [i_f]_{ABC} dt + [v_f]_{ABC} \quad (7)$$

Differentiate the above equation,

$$\frac{d[v_S]_{ABC}}{dt} = \frac{d[i_f]_{ABC}}{dt} * r + \frac{d^2[i_f]_{ABC}}{dt^2} * L + \frac{1}{c}[i_f]_{ABC} + \frac{d[v_f]_{ABC}}{dt} \quad (8)$$

By using the dq transform,

$$\begin{bmatrix} i_{fA} \\ i_{fB} \\ i_{fC} \end{bmatrix} = \begin{bmatrix} \sin\omega t & \cos\omega t \\ \sin(\omega t - 120) & \cos(\omega t - 120) \\ \sin(\omega t - 240) & \cos(\omega t - 240) \end{bmatrix} \begin{bmatrix} i_{fd} \\ i_{fq} \end{bmatrix} \quad (9)$$

$$\frac{dv_{Sd}}{dt} = r\left(\frac{di_{fd}}{dt} - \omega i_{fq}\right) + L\left(\frac{d^2 i_{fd}}{dt^2} - 2\omega * \frac{di_{fq}}{dt} - \omega^2 i_{fd}\right) + \frac{i_{fd}}{c} + \frac{dv_{fd}}{dt} - \omega v_{fq} \quad (10)$$

Taking the Laplace transform and used the small signal analysis, then the equation become,

$$S\frac{\Delta v_{Sd}}{\omega} = \Delta i_{fd}\left[S^2\frac{L}{\omega} + S\frac{r}{\omega} + \left(\frac{1}{\omega c} - \omega L\right)\right] + \Delta i_{fq}(S2L + r) - \Delta v_{fq} + S\frac{\Delta v_{fd}}{\omega} \quad (11)$$

The change of filter current is described as,

$$\Delta i_{fd} = \frac{\Delta v_{fq} * \frac{\omega}{L}}{S^2 + S\frac{r}{L} + \frac{1}{Lc}} - \frac{\Delta i_{fq} * \frac{\omega}{L}(S2L + r)}{S^2 + S\frac{r}{L} + \frac{1}{Lc}} - \frac{S\frac{\Delta v_{fd}}{L}}{S^2 + S\frac{r}{L} + \frac{1}{Lc}} + \frac{S\frac{\Delta v_{sd}}{L}}{S^2 + S\frac{r}{L} + \frac{1}{Lc}} \quad (12)$$

By eliminating the disturbances then the filter current is described as,

$$\Delta i_{fd} = \frac{\Delta v_{fq} * \frac{\omega}{L}}{S^2 + S\frac{r}{L} + \frac{1}{Lc}} \quad (13)$$

The active current injected into grid is described as,

$$i_{fd} = \left(\frac{P_{grid}/3}{v_S/\sqrt{3}}\right)\sqrt{2} \quad (14)$$

3.5. Control of Harmonic Current

The harmonic current from source is compensated by BCMO approach. Generally, the harmonic current is controlled by the proportional controller [35-36]. Though, reference signals are not tracked by this controller. Here, the BCMO approach with grid current feedback is proposed to control the harmonics of the system. Though, need the load and grid current as well as passive impedance given to control loop. The PID controller is utilized to minimize the steady state error as well as bandwidth of closed loop control. Fig 4 illustrates the harmonic current control loop.

DOI : https://doi.org/10.56452/7-8-41

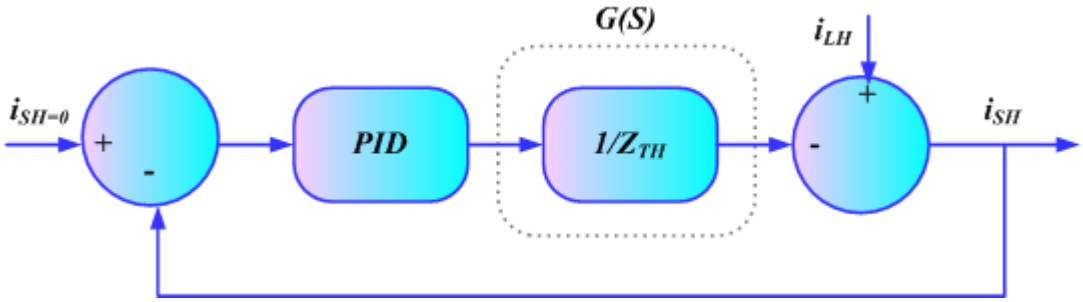

Fig 4: Harmonic current control loop

Consider the reference current as zero because the harmonic currents of the grid must be zero in hybrid active filter. The harmonic current control loop and the open loop transfer function are described by,

$$G(S) = \frac{1}{Z_F H(S)} = \frac{\frac{S}{L}}{S^2 + S\frac{r}{L} + \frac{1}{Lc}} \tag{15}$$

Through given the delay phase angle before resonant frequency as well as top phase angle after resonant frequency, the steady state error is minimized using the proposed approach with PID controller. The transfer function is described as,

$$G_C(S) = K_P * \frac{\left(1 + \frac{S}{\omega_Z}\right)}{\left(1 + \frac{S}{\omega_P}\right)} * \frac{(1 + \omega_L)}{S} \tag{16}$$

4. Assessment of Power Quality Based on Issues

In this section major power quality queries like voltage imbalance, voltage rise and harmonic distortion are described.

4.1. Voltage Unbalance

The voltage or current imbalance is known as the level of other change in magnitude of voltages, currents of phases, deviation. Hence unbalance of the voltage is recognized by 1 or 2 lines of a 3-phase system, over the transmission lines, and asymmetrical distribution of converters. Due to the overheating of transformer also produce the unbalance voltage. It affects the performance as well as reduce the efficiency of the system. Estimation of voltage imbalance calculates the amplitude and phase of the nodal voltages with the feeder through which load flow is determined.

4.2. Voltage Rise

One of the important factors which affect the voltage regulation is voltage increase issue. Typically, the distribution networks were modeled depending on downstream flow of energy from the transmitting line to distributing line, providing power to passive consumers. The voltage variation control is mainly in the voltage associated with the feeder. The controller is used to change the downstream power flow which changes the voltage profile of the feeder. When the generation demand exceeds the feed requirement and more power is pumped again into the upstream phase then the problems are arising. This repeated power flow causes voltage rise (VR) afar acceptable limits across the feeder. The voltage drop is described as,

$$\Delta\vec{E} = \vec{E}_m - \vec{E}_n = i(R + jX) = \Delta\vec{E}_{real} + \Delta\vec{E}_{imag} \tag{17}$$

Consider the relation of active and reactive power,

$$\left|\Delta\vec{E}\right| \approx \left|\Delta\vec{E}_{real}\right| = \frac{r.P_r + XQ_r}{\left|\Delta\vec{E}_n\right|} \tag{18}$$

DOI : https://doi.org/10.56452/7-8-41

4.3. Power loss

Through peak load conditions distribution systems build up instability which provides restriction violations. The power loss is must controlled for the quality of power is increase. The loss of distribution system is described by,

$$P_{loss}^{\ D} = \sum_{i=1}^{N}\sum_{j=1}^{N}\left[\alpha_{ij}(p_i p_j + q_i q_j) + \chi_{ij}(q_i p_j - p_i q_j)\right] \tag{19}$$

here,

$$\alpha_{ij} = \frac{r_{ij}}{V_i V_j}\cos(\delta_i - \delta_j) \tag{20}$$

$$\chi_{ij} = \frac{r_{ij}}{V_i V_j}\sin(\delta_i - \delta_j) \tag{21}$$

Here distribution side exact loss is denoted as $P_{Loss}^{\ D}$; resistance among bus i and bus j is denoted as r_{ij}, voltage magnitude bus i and j is denoted as V_i and V_j correspondingly, voltage angle in bus i is denoted as δ_i, voltage angle in bus j is denoted as δ_j, actual and reactive power injection in bus i is denoted as p_i and q_i, the actual and reactive power injection in bus j is denoted as p_j and q_j.

4.4. Voltage deviation

In the distribution network the management of voltage is important factor. The voltage profile is varied based on the voltage deviation. In the distribution system, each bus is evaluating the voltage of the system. The DG placed in the distribution system provides voltage profile improvement and stableness of the system. Equations of voltage deviation is,

$$v_d = \sum_{i=1}^{N}\left(\frac{v_i - v_{sp}}{v_{sp}}\right) \tag{22}$$

Here, voltage specified is denoted as v_{sp}, voltage magnitude bus i is denoted as v_i.

4.5. Load balancing

For balance the load of the bus lines is the important aspects. The load balancing is calculated by,

$$V = \sum_{i=1}^{N}\left(\frac{i_i}{i_L^{avg}}\right) \tag{23}$$

Where, current of branch i is denoted as i_i, the branch current of the system does not go the limit. it is described as $i_i \le i_i^{rd}$, The total line average current is described as,

$$I_N^{avg} = \sum_{L=1}^{N}\left(\frac{i_L}{N}\right) \tag{24}$$

Here, total number of lines is denoted as N.

4.6. Voltage and current harmonic distortion

Due to the passive as well as active nonlinear devices, the power system produces harmonics. Total voltage and current harmonic distortion is used for determine the harmonic performance of the bus system. The total voltage harmonic distortion contains the ratio of the sum of power of all harmonic voltage components to the power of the fundamental voltage frequency. The whole current harmonic distortion contains the ratio of the sum of power of all harmonic current components to the power of the fundamental current frequency.

$$TVHD = \frac{100 \times \sqrt{v_{rms}^2 - v_{frms}^2}}{v_{frms}} \tag{25}$$

DOI : https://doi.org/10.56452/7-8-41

$$TIHD = \frac{100 \times \sqrt{i_{rms}^2 - i_{frms}^2}}{i_{frms}} \tag{26}$$

Here, TVHD denots total voltage harmonic distortion, $TIHD$ denotes total current harmonic distortion, v_{frms} denotes fundamental voltage frequency, i_{frms} denotes fundamental current frequency, v_{rms} denotes harmonic voltage component, i_{rms} denotes harmonic current component.

5. Proposed HUA-BCMO Approach Based Power Quality Improvement

HUA-BCMO approach was suggested for controlling the active power to compensates harmonic current. The proposed approach made of APC and HCC. At first, active power control is performed using the HUA approach. After that, BCMO approach is used for harmonic compensation. The loops are utilized the PI controllers for control the current and power. Power converter is controlled by harmonics and is compensated by voltage-mode control. Compensate voltage is created using power converter which was converted into compensating current to facilitate the filter harmonic currents are created as non-linear loads. Hence considered the feedback as a harmonic currents to grid, references to grid harmonic currents below the ideal condition.

5.1. Active Power Control Based on HUA Approach

One of the metaheuristic algorithms is Human urbanization algorithm that is inspired by the qualities of human urbanization for maximize the life positions. Because of circumstances and growth of cities, many people are moving their [37]. HUA approach is based on the better surroundings of the cities. Journey, immigrate; depopulation and exposure are some of the urbanism affecting factors. Adventuring are defined as motion for exploring new areas depend on the preceding experiences and random motions Migrations are alterations of livelihood change from a town to other town by calculating the luxuries. Populations were known by various routes that are open to towns. In the lookup every output is assumed as possible result. In the manuscript, HUA method was for controlling the APC loop and this active power is controlled by PI controller. The stride methods of HUA algorithm is described below,

Step 1: Initialization

In this process, input parameters are known by load current, dc link voltage, source voltage, proportional and integral gain constants in the PI controller are used.

Step 2: Random Generation

In this stage, the initialized parameters are randomly generated.

$$D = \begin{bmatrix} K_{pt}^{11} K_{it}^{11} & K_{pt}^{12} K_{it}^{12} & \cdots & K_{pt}^{1n} K_{it}^{1n} \\ K_{pt}^{21} K_{it}^{21} & K_{pt}^{22} K_{it}^{22} & \cdots & K_{pt}^{2n} K_{it}^{2n} \\ \vdots & \vdots & \vdots & \vdots \\ K_{pt}^{m1} K_{it}^{m1} & K_{pt}^{m2} K_{it}^{m2} & \cdots & K_{pt}^{mn} K_{it}^{mn} \end{bmatrix} \tag{27}$$

Step 3: Fitness Evaluation

The fitness is calculated based on objective function of reduction of error value, which is described as,

$$Fitness_j = Min\ Error(x) \tag{28}$$

The error is described as,

$$Error_P(x) = i_{fd}^{ref} - i_{fd}^{a} \tag{29}$$

Step 4: Position Updation using HUA

Using the following equation the city population like HUA method was reorganized as fitness

$$P_i(t+1) = P_i(t) + Index_j \tag{30}$$

Where, index of city specifies $Index_j$

DOI : https://doi.org/10.56452/7-8-41

Step 5: Determine the Radius of the City
The city radius is established in below equation,

$$R_i = \frac{k * D * R}{P_i} \tag{31}$$

Where, the radius of the city i specifies R_i, Population of city i specifies P_i, and the iteration specifies k. The variable D measured and it depends upon the quality of city center comparedto the city capital. Variable D is measured as,

$$D = arc\tan\left(\left|\frac{(F(capi) - F(dis\,cent))}{F(capi)}\right|\right) + 0.5 \tag{32}$$

Where, the distance from the city centre specifies $F(dis\,cent)$

Step 6: Determine the Optimal Location
Step 6 shows, the parameters, that are already defined from the city center and the value is stored and are fragmented. By using these values the best active power are identified and the parameter is set to capital. Hence, step three and four is continued for each iteration.

Step 7: Termination Criteria
Series are checked to attain the highest level, if not reached its optimal solution, repeat the process again until the desired solution is found.

5.2. Harmonic Current Control Based on Balancing Composite Motion Optimization (BCMO)
Balancing Composite Motion Optimization is the population-based optimization approaches that are utilized for balancing the composite motion characteristic of individuals in result space [38-40]. The candidate solution is determined by the global optimal region. At first, create the candidate solutions randomly by S space via few heuristic conditions. According to the physical perspective, the candidates solutions are assumed as particles as well as heuristic conditions are the composite in a physical space. In the manuscript, the harmonic current is controlled by this BCMO approach. Harmonic compensation of power converters are control by voltage-mode control. Compensate voltage is generated by the power converter which are converted to compensate the current to filter the harmonic current created as nonlinear loads. Hence, the reference is considered as grid harmonic currents and the real-time harmonic currents of grid is considered as the feedback. Step by step process of BCMO approach are described below,

Step 1: Initialization
Initialize the population distribution in the solution space like upper and lower boundaries of ith individuals, dimensional vector, gain parameters of the PID controller, grid current, and feedback current.

Step 2: Random Generation
After the starting process, randomly generate the initial parameters using below equation,

$$X_i = X_i^l + ra(1, D) \times \left(X_i^u - X_i^l\right) \tag{33}$$

Here, X_i^u and X_i^l is the upper and lower boundaries for ith individuals. D is the dimensional vector.

Step 3: Fitness Function
Compute the fitness function for all iteration which can be expressed as,

$$F_t = Min(thd) \tag{34}$$

Step 4: Finding Instant Global Point
Initially, all the individuals are located in the different region. The instant global point can be determined using the following equation,

DOI : https://doi.org/10.56452/7-8-41

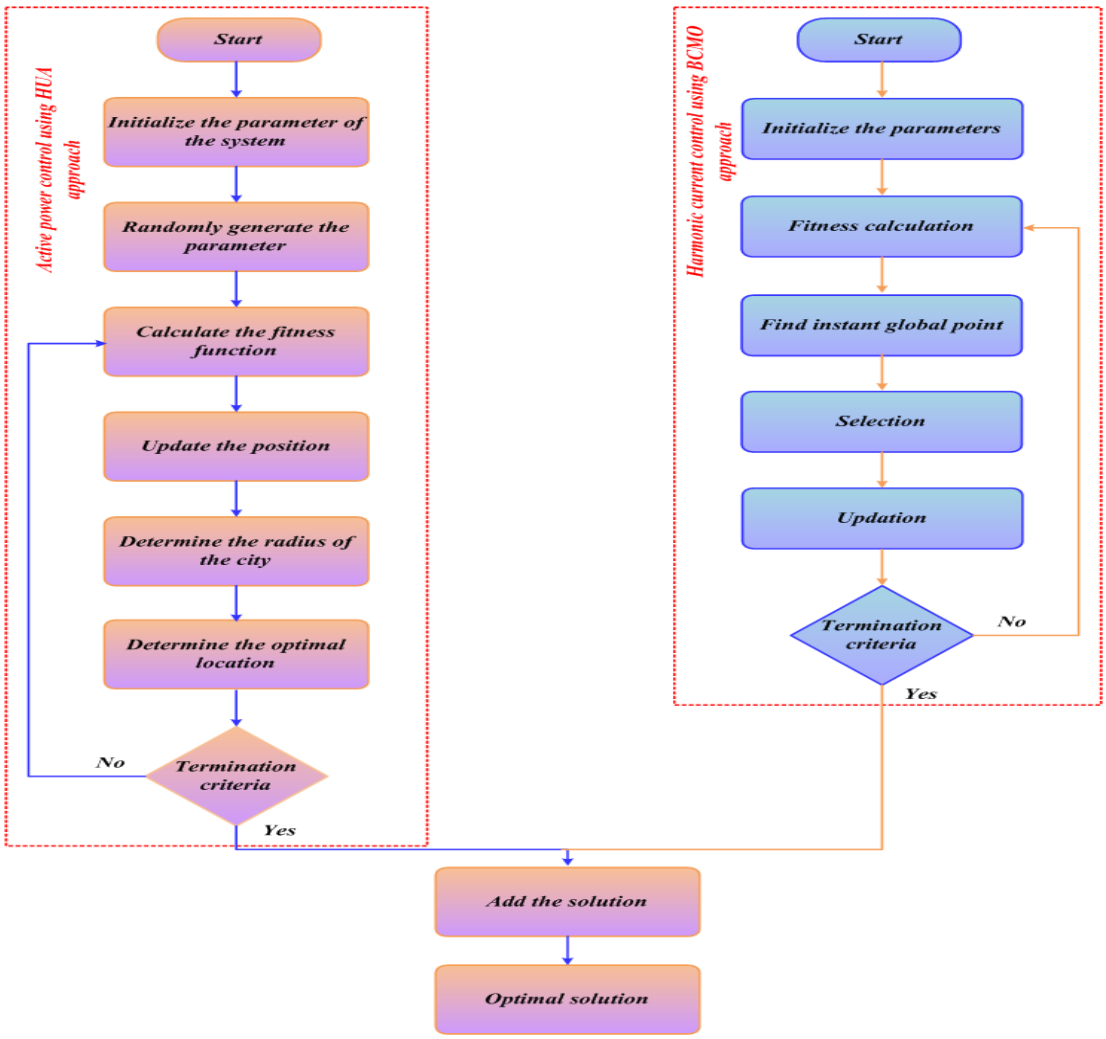

Fig: 5: Flowchart of the HUA-BCMO approach

$$x_O = \begin{cases} U_1^T \ if \ F\left(U_1^T\right) < F\left(X_1^{T-1}\right) \\ X_1^{T-1} \ else \end{cases} \tag{35}$$

Step 5: Selection

The individual with best objective function value is selected to move on S space for finding the optimal solution.

Step 6: Updation

After the selection process, update the upper and lower boundaries in all iteration.

Step 7: Termination

If the process reaches the objective condition, it will be terminated otherwise it continuing from step 3.

6. Result and Discussions

In this section the simulation outcome is described based on the performance of the proposed method. To improve the quality of power, this manuscript uses hybrid HUA-BCMO approach. The HUA approach is used to control the active power of the PV system and the BCMO approach is used to control harmonics at the load side. At last, the suggested approach is simulated by MATLAB Simulink Platform. The suggested approach increases the quality of the power and reduces the harmonics in effective manner. The suggested approach is analyzed based on the source active and reactive power and load active and reactive power, source current and

DOI : https://doi.org/10.56452/7-8-41

load current. The outcome of suggested method is likened to the existing approaches such as tree seed algorithm (TSA), Salp swarm algorithm (SSA) and Particle Swarm Optimization (PSO).

Fig 6 represents the analysis of source current and source voltage. The current source is oscillating among the time period -1.5×10^4 A to 1.5×10^4 A at 0 to 0.198sec. Next the, present level increased and oscillating among the range of -1.6×10^4 A to 1.6×10^4 A at 0.199 to 0.31 sec the time period. Again, the current is oscillating among-1.5×10^4 A to 1.5×10^4 A at 0.32 to 0.5 sec time period . Analysis of source active power is shown in fig 7. At first the active power is 0 at 0 to 0.02 sec period of time. Then the active power is raised to 0 to 2.8×10^4 W at 0.02 sec time period and it is constant to 2.8×10^4 W at 0.02 to 0.2 sec period of time . After that, small oscillations are occurring at the period of 0.21 sec and then the power is increased to 2.9×10^4 W at the period of 0.22 to 0.31 sec. After that, the power is oscillated at the period of 0.31 to 0.325 sec. Again it is constant to 2.8×10^4 W at 0.33 to 0.5 sec period of time . Fig 8 shows reactive power analysis from the orgin start at 0 and it decreased to reach -9500 kVar at 0.02sec time period. Next, the reactive power is steady to-9500 kVar at the time period 0.02 to 0.2 sec. Then the reactive power is oscillated at small value (-9400 kVar) at the period of 0.201 to 0.22 sec. Again it is constant to -9500 kVar at 0.221 to 0.31 sec time period. After that, it oscillated a small value (-10000 kVar) at 0.31 to 0.33 sec time period. At the period of 0.33 to 0.5 sec, the reactive power is -9500 kVar. Analysis of comparison of source active power based on proposed and existing approach is illustrated in fig 9. By comparing the period of 0.2 to 0.21 sec, the active power of proposed approach is start at 2.75×10^4 W and it increased to reach 2.77×10^4 W at 0.205 sec. The active power of TSA, SSA, and PSO approach at 0.205 sec is 2.78×10^4 W, 2.801×10^4 W, and 2.84×10^4 W respectively. From this comparison, it is conclude that, the suggested approach active power are lower than existing approaches. That means, the harmonics of the proposed system is less than the existing approach is proved. Analysis of comparison of source reactive power based on proposed and existing method is illustrated in fig 10. By comparing the period of 0.2 to 0.21 sec, the reactive power of proposed approach is start at -9000 kVar and it increased to reach -8800 kVar at 0.205 sec. The reactive power of TSA, SSA, and PSO approach at 0.205 sec is -8300 kVar, -7800 kVar and -6300 kVar respectively. From this comparison, it is conclude that, the suggested approach reactive power is low than existing approaches. That means, the utilization of proposed approach provides less harmonics than the existing approach is proved.

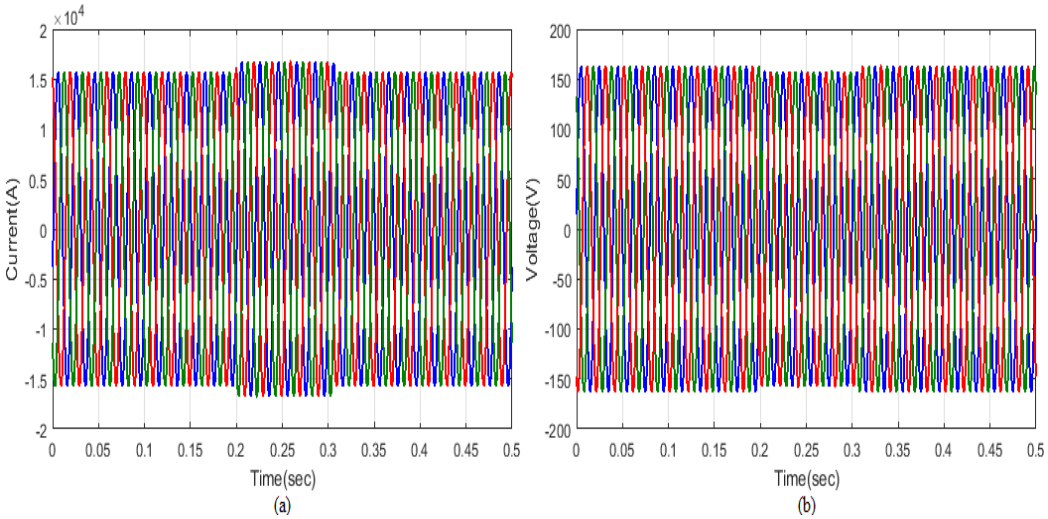

Fig 6: Analysis of source current and source voltage

DOI : https://doi.org/10.56452/7-8-41

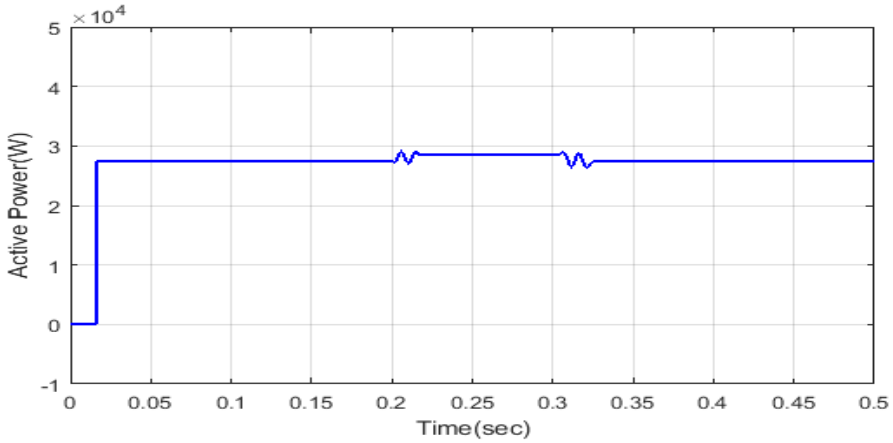

Fig 7: Analysis of source active power

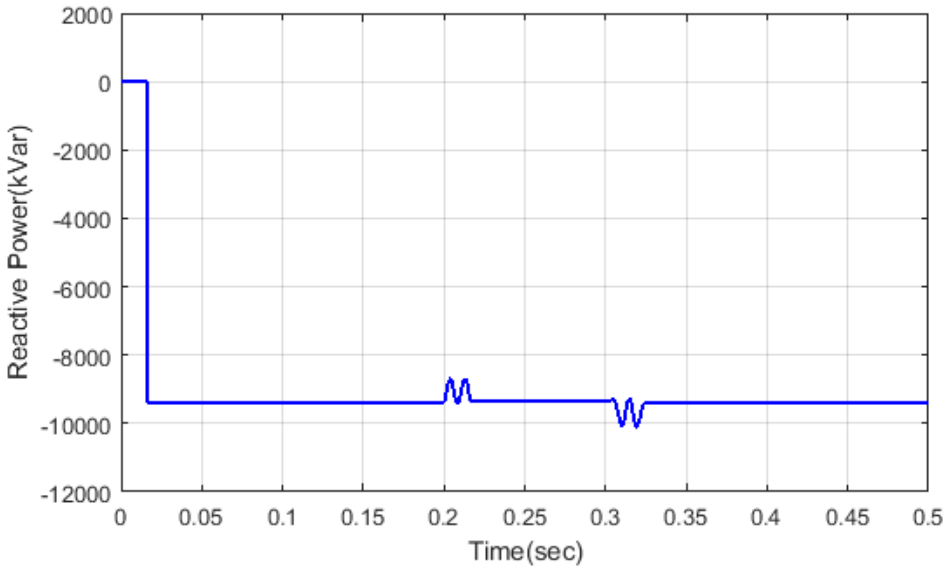

Fig 8: Analysis of source reactive power

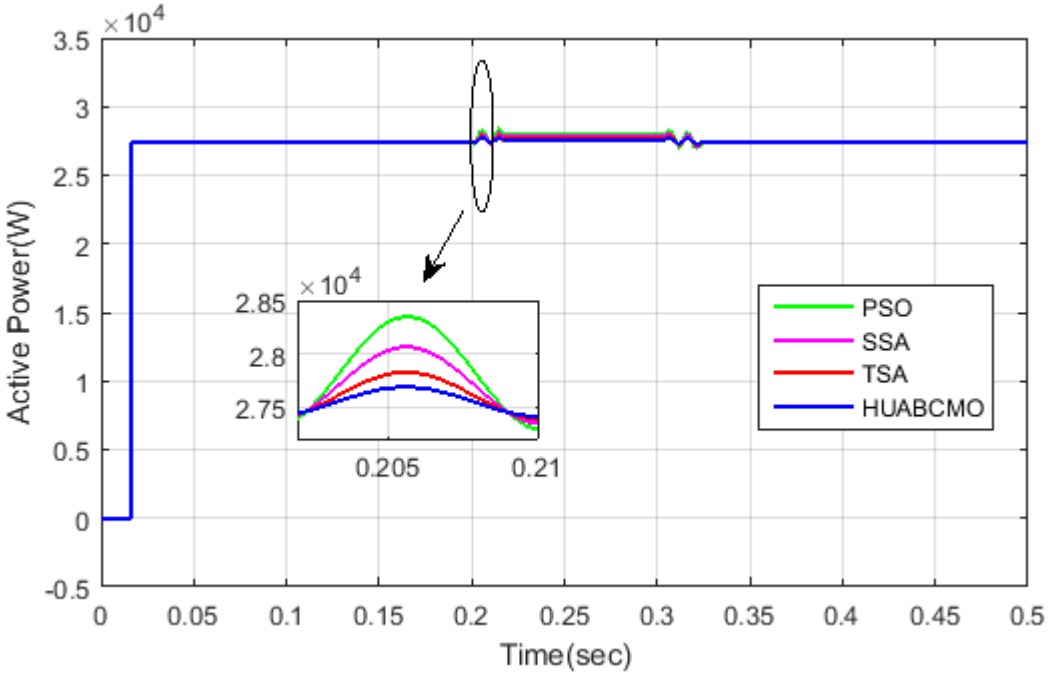

DOI : https://doi.org/10.56452/7-8-41

Fig 9: Analysis of comparison of source active power based on proposed and existing approach

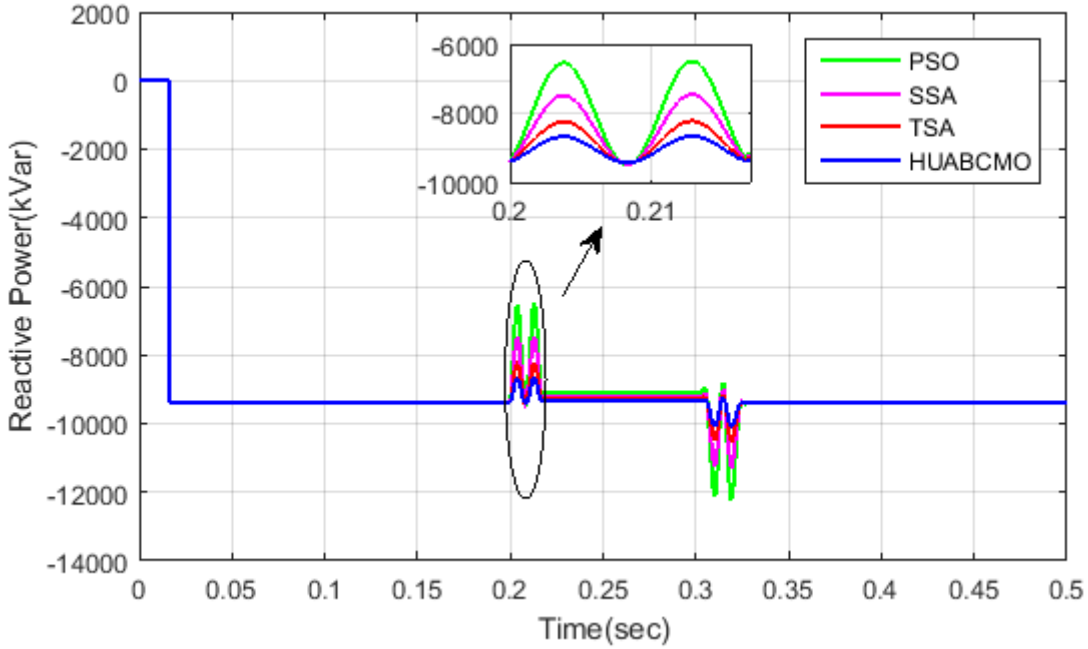

Fig 10: Analysis of comparison of source reactive power based on proposed and existing approach

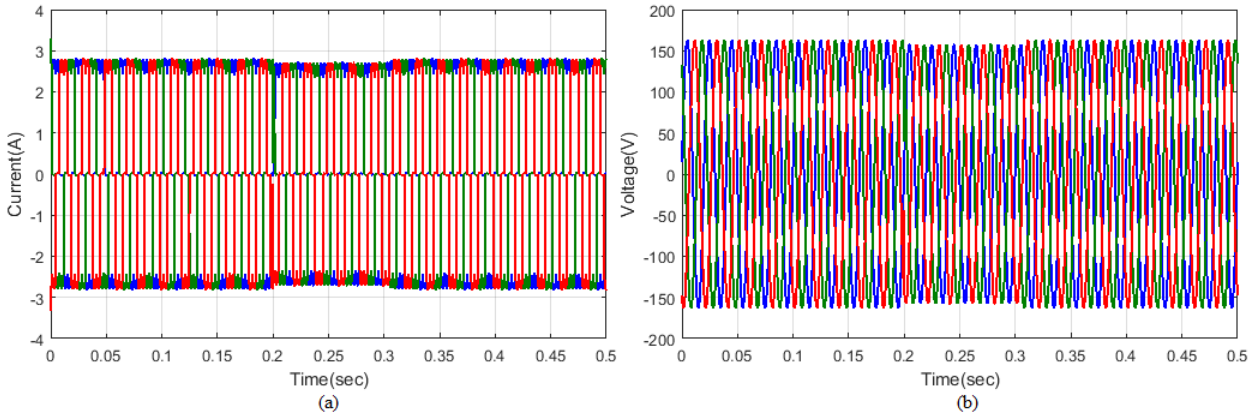

Fig 11: Analysis of (a) Load current (b) Load voltage

DOI : https://doi.org/10.56452/7-8-41

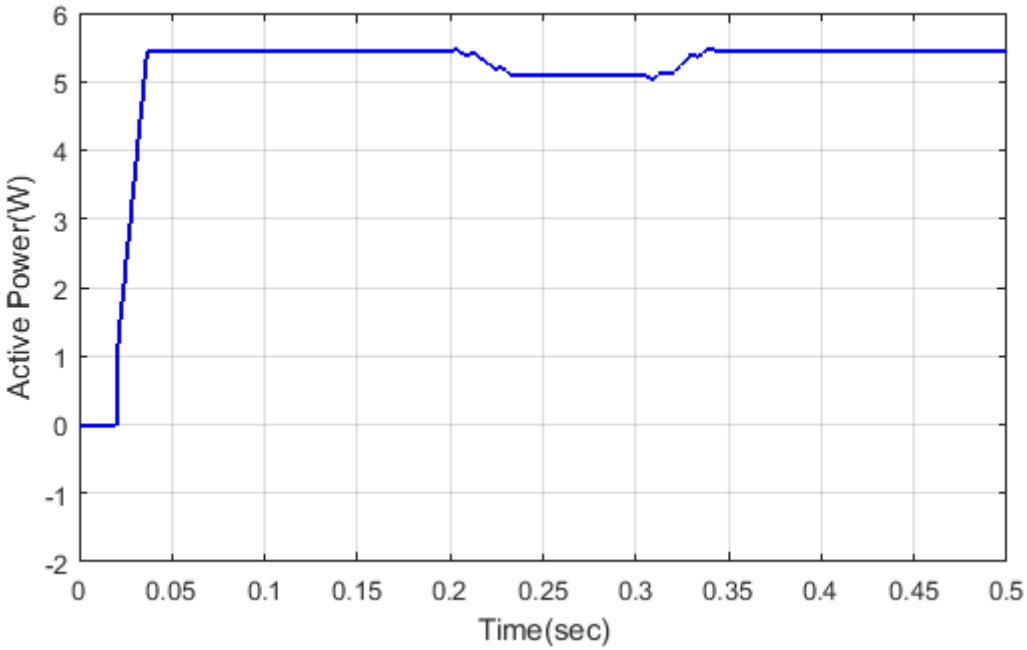

Fig 12: Analysis of load active power

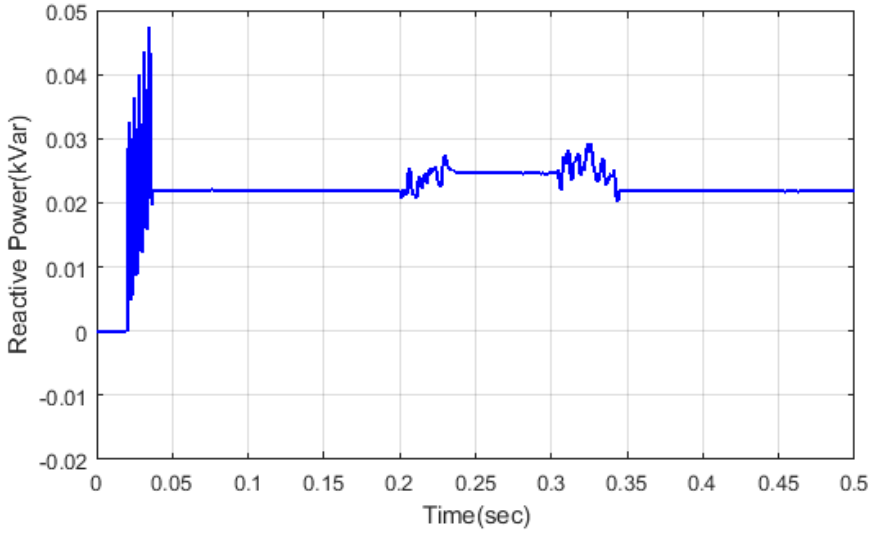

Fig 13: Analysis of load reactive power

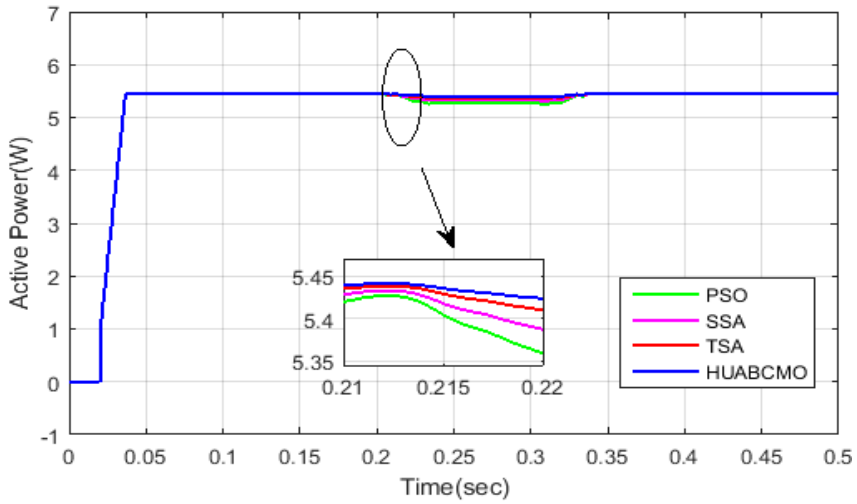

Fig 14: Analysis of comparison of load active power of proposed and existing approaches

DOI : https://doi.org/10.56452/7-8-41

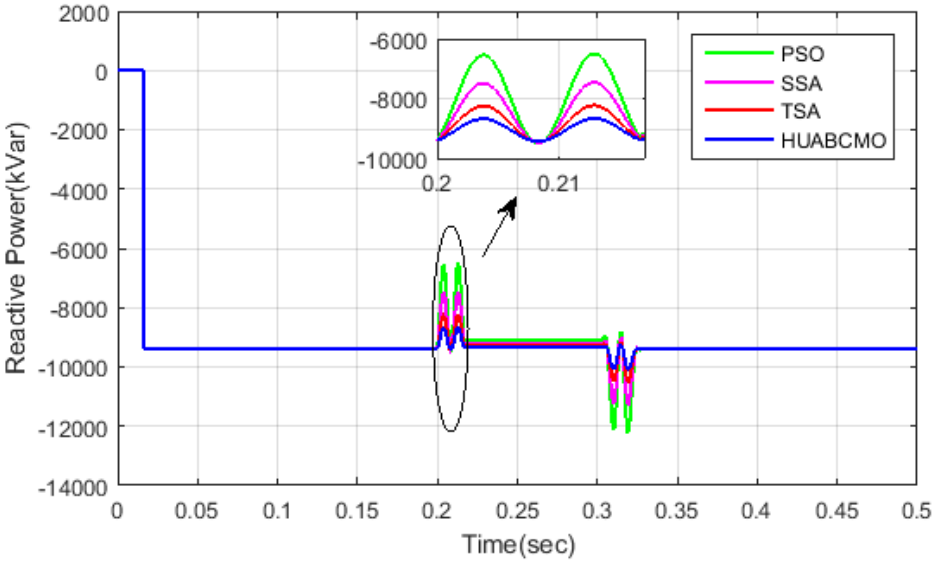

Fig 15: Analysis of comparison of load reactive power of proposed and existing methods

Analyzing the current and voltage of load using proposed approach is illustrated in fig 11. Analysis of load current is depicting in fig 11 (a). The load current is oscillating among -2.8 A to 2.8 A at the period of 0 to 0.2 sec. Then the load current is slightly decreased to oscillate among -2.7 A to 2.7 A at the period of 0.2 to 0.31 sec. Again, the load current is oscillate among -2.8 A to 2.8 A at the period of 0.31 to 0.5 sec. In fig 11 (b) the analysis of load current is shown. The load voltage is varying from -160 to 160 V at the period of 0 to 0.2 sec. Then the load voltage is slightly decreased to reach -165 to 165 V at the period of 0.2 to 0.31 sec. Again the voltage is varying from -160 to 160 V at the period of 0.31 to 0.5 sec. Analysis of load active power was illustrated in fig 12. Active power of load are initially zero at 0 to 0.025 sec period of time. Then, the active power is increased to reach 5.5 W at the time period of 0.04 sec. After that, it is constant to 5.5 W at the time period of 0.04 to 0.2 sec. Next, it is slightly reduced to 5.1 W at 0.23 sec and it is maintained to constant until 0.3 sec. Later, it raised to attain 5.5 W at 0.34 sec period. At o.34 to 0.5 sec, the active power is constant to 5.5 W. Analysis of load reactive power is shown in fig 13. The reactive power is initially zero at 0 to 0.02 sec, and then the reactive power is oscillated up to 0.048 kVar at 0.02 to 0.03 sec time period. After that it is constant to 0.021 kVar at 0.03 to 0.2 sec time period , and then small oscillations are present in the period of 0.201 to 0.23 sec. After that, it is constant to 0.025 kVar at 0.23 to 0.301 sec time period . Again some oscillations are present at 0.301 to 0.34 sec time period. Next, the reactive power of load is 0.021 kVar at 0.34 sec time period, and it is constant up to 0.5 sec. Analysis of comparison of load active power of proposed and existing approaches is shown in fig 14. For analysis, 0.21 to 0.22 sec time period, the proposed approach active power is high than the existing approaches. The proposed approach active power is 5.43 W at 0.22 sec time period , at the same time the existing approach such as TSA, SSA, and PSO active power values becomes5.41 W, 5.38 W, and 5.36 W respectively. From fig 14, we conclude that, proposed method load active power is high than the existing approach, that means, at the sag condition, the proposed approach provide better outcome than the existing approaches. Analysis of comparison of load reactive power of proposed and existing approaches is shown in fig 15. For analysis, the proposed approach reactive power is less than the existing approaches of 0.2 to 0.21 sec time period. The proposed approach reactive power is -8500 kVar at the time period of 0.205 sec and at the same time the existing approaches like TSA,SSA and PSO reactive power values becomes -8200 kVar, -7500 kVar, and -6500 kVar respectively. From fig 15, we conclude that, proposed approach load reactive power is low than the existing approach, that means, at the harmonics condition, the proposed approach provide better outcome than the existing approaches.

Table 1: Comparative analysis of source active power of proposed and existing approaches at harmonics condition

Time	Source active power of proposed approach	Source active power based on TSA approach	Source active power based on SSA approach	Source active power based on PSO approach

DOI : https://doi.org/10.56452/7-8-41

0.2	2.75×10^4 W	2.75×10^4 W	2.75×10^4 W	2.75×10^4 W
0.202	2.76×10^4 W	2.765×10^4 W	2.77×10^4 W	2.78×10^4 W
0.205	2.77×10^4 W	2.78×10^4 W	2.81×10^4 W	2.84×10^4 W
0.208	2.75×10^4 W	2.76×10^4 W	2.77×10^4 W	2.78×10^4 W
0.21	2.74×10^4 W	2.738×10^4 W	2.737×10^4 W	2.736×10^4 W

Table 2: Comparative analysis of source reactive power of proposed and existing approaches at harmonics condition

Time	**Source reactive power of proposed approach**	**Source reactive power based on TSA approach**	**Source reactive power based on SSA approach**	**Source reactive power based on PSO approach**
0.2	-9100 kVar	-9100 kVar	-9100 kVar	-9100 kVar
0.202	-8800 kVar	-8300 kVar	-8250 kVar	-8200 kVar
0.205	-8700 kVar	-8100 kVar	-7500 kVar	-6500 kVar
0.208	-9100 kVar	-9100 kVar	-9100 kVar	-9100 kVar
0.21	-9080 kVar	-9070 kVar	-9065 kVar	-9060 kVar

DOI : https://doi.org/10.56452/7-8-41

Table 3: Comparative analysis of load active power of proposed and existing approaches at harmonics condition

Time	Load active power of proposed approach	Load active power based on TSA approach	Load active power based on SSA approach	Load active power based on PSO approach
0.21	5.44 W	5.438W	5.435 W	5.43 W
0.215	5.437 W	5.436 W	5.43 W	5.4 W
0.218	5.436 W	5.435 W	5.4 W	5.38 W
0.22	5.43 W	5.42 W	5.39 W	5.36 W

Table 4: Comparative analysis of load reactive power of proposed and existing approaches at harmonics condition

Time	Load reactive power of proposed approach	Load reactive power based on TSA approach	Load reactive power based on SSA approach	Load reactive power based on PSO approach
0.2	-9200 kVar	-9200 kVar	-9200 kVar	-9200 kVar
0.202	-8900 kVar	-8200 kVar	-8100 kVar	-8000 kVar
0.205	-8800 kVar	-8100 kVar	-7500 kVar	-6500 kVar
0.208	-9100 kVar	-9100 kVar	-9100 kVar	-9100 kVar
0.21	-9000 kVar	-8990 kVar	-8980 kVar	-9970 kVar

Comparative analysis of source active power of suggested and existing approaches at harmonics condition is tabulated in table 1. Here, the proposed approach and the existing approaches like TSA, SSA, and PSO approach are compared. From this analysis, it is conclude that, the proposed approach active power under harmonics condition is less than the existing approaches. Comparative analysis of source reactive power of proposed and existing approaches at harmonics condition is tabulated in table 2. Here, the proposed approach and the existing approaches like TSA, SSA, and PSO approach are compared. From this analysis, it is conclude that, the proposed approach reactive power under harmonics condition is less than the existing approaches. Comparative analysis of load active power of proposed and existing approaches at harmonics condition is tabulated in table 3. Here, the proposed approach and the existing approaches like TSA, SSA, and PSO approach are compared. From this analysis, it is conclude that, the proposed approach active power under harmonics condition is high than the existing approaches. Comparative analyses of proposed and existing approaches of load reactive power at harmonics condition are tabulated in table 4. Here, the proposed approach and the existing approaches like TSA, SSA, and PSO approach are compared. From this analysis, it is conclude that, the proposed approach reactive power under harmonics condition is less than the existing approaches.

7. Conclusion

In this manuscript, hybrid HUA-BCMO method is suggested for improving the power quality of three-phase grid-connected by solar photovoltaic system using single-phase solar inverter. Hence the single power is supplying from direct voltage source to ac grid system. In the proposed approach, there are two controls are utilized: (1)Active current control,(2)harmonic current control. HUA approach is performing the active control of the system and the harmonic control is performed by the BCMO approach. Using this approaches effectively control the active power and reduce the harmonics efficiently through which increase the quality of the power. The proposed method is simulated as MATLAB Simulink platform. Under this proposed approach, source current and voltage, load current voltage, reactive and active power is analyzed. The proposed approach and the existing approaches like TSA, SSA, and PSO approach are compared. From the analysis, we conclude the efficiency of the proposed approach are high and ripple current of the inverter is very less and the proposed approach provide high active power at the load side is proved.

References

[1] E. Koutroulis, K. Kalaitzakis and N. Voulgaris, "Development of a microcontroller-based, photovoltaic maximum power point tracking control system", IEEE Transactions on Power Electronics, vol. 16, no. 1, pp. 46-54, 2001.

[2] Y. Chen and K. Smedley, "A Cost-Effective Single-Stage Inverter With Maximum Power Point Tracking", IEEE Transactions on Power Electronics, vol. 19, no. 5, pp. 1289-1294, 2004.
[3] S. Chung, "Phase-locked loop for grid-connected three-phase power conversion systems", IEE Proceedings - Electric Power Applications, vol. 147, no. 3, p. 213, 2000.
[4] J. Selvaraj and N. Rahim, "Multilevel Inverter For Grid-Connected PV System Employing Digital PI Controller", IEEE Transactions on Industrial Electronics, vol. 56, no. 1, pp. 149-158, 2009.
[5] ChongmingQiao and K. Smedley, "Three-phase unity-power-factor star-connected switch (VIENNA) rectifier with unified constant-frequency integration control", IEEE Transactions on Power Electronics, vol. 18, no. 4, pp. 952-957, 2003.
[6] R. Kadri, J. Gaubert and G. Champenois, "Nondissipative String Current Diverter for Solving the Cascaded DC–DC Converter Connection Problem in Photovoltaic Power Generation System", IEEE Transactions on Power Electronics, vol. 27, no. 3, pp. 1249-1258, 2012.
[7] A. Abramovitz, B. Zhao and K. Smedley, "High-Gain Single-Stage Boosting Inverter for Photovoltaic Applications", IEEE Transactions on Power Electronics, vol. 31, no. 5, pp. 3550-3558, 2016.
[8] D. Alexa and A. Sirbu, "Optimized combined harmonic filtering system", IEEE Transactions on Industrial Electronics, vol. 48, no. 6, pp. 1210-1218, 2001.
[9] S. Srianthumrong and H. Akagi, "Medium-voltage transformerless ac/dc power conversion system consisting of a diode rectifier and a shunt hybrid filter", IEEE Transactions on Industry Applications, vol. 39, no. 3, pp. 874-882, 2003.
[10] J. Klima, J. Tlusty, J. Skramlik and V. Valouch, "Analytical model and investigation of a four-switch space-vector modulated hybrid power filter with six-fold switching symmetry", Renewable Energy and Power Quality Journal, vol. 1, no. 07, pp. 54-59, 2009.
[11] J. Wu, H. Jou, Y. Feng, W. Hsu, M. Huang and W. Hou, "Novel Circuit Topology for Three-Phase Active Power Filter", IEEE Transactions on Power Delivery, vol. 22, no. 1, pp. 444-449, 2007.
[12] R. Bojoi, L. Limongi, D. Roiu and A. Tenconi, "Enhanced Power Quality Control Strategy for Single-Phase Inverters in Distributed Generation Systems", IEEE Transactions on Power Electronics, vol. 26, no. 3, pp. 798-806, 2011.
[13] C. Pazhanimuthu and S. Ramesh, "Grid integration of renewable energy sources (RES) for power quality improvement using adaptive fuzzy logic controller based series hybrid active power filter (SHAPF)", Journal of Intelligent & Fuzzy Systems, vol. 35, no. 1, pp. 749-766, 2018.
[14] A. Blorfan, J. Mercklé, D. Flieller, P. Wira and G. Sturtzer, "Sliding Mode Controller for Three-Phase Hybrid Active Power Filter with Photovoltaic Application", Smart Grid and Renewable Energy, vol. 03, no. 01, pp. 17-26, 2012.
[15] Y. Chaibi, A. Allouhi, M. Salhi and A. El-jouni, "Annual performance analysis of different maximum power point tracking techniques used in photovoltaic systems", Protection and Control of Modern Power Systems, vol. 4, no. 1, 2019.
[16] S. Farghal, M. Kandil and A. Elmitwally, "Evaluation of a shunt active power conditioner with a modified control scheme under nonperiodic conditions", IEE Proceedings - Generation, Transmission and Distribution, vol. 149, no. 6, p. 726, 2002.
[17] S. Swain, P. Ray and K. Mohanty, "Improvement of Power Quality Using a Robust Hybrid Series Active Power Filter", IEEE Transactions on Power Electronics, vol. 32, no. 5, pp. 3490-3498, 2017.
[18] C. Young, M. Chen and C. Ko, "High power factor transformerless single-stage single-phase ac to high-voltage dc converter with voltage multiplier", IET Power Electronics, vol. 5, no. 2, p. 149, 2012.
[19] Y. Panov, J. Cho and F. Lee, "Zero-voltage-switching three-phase single-stage power factor correction convertor", IEE Proceedings - Electric Power Applications, vol. 144, no. 5, p. 343, 1997.
[20] S. Mohammad Noor, A. Omar and M. Radzi, "Single-Phase Single Stage String Inverter for Grid Connected Photovoltaic System", Applied Mechanics and Materials, vol. 785, pp. 177-181, 2015.
[21] S. Echalih, A. Abouloifa, I. Lachkar, J. Guerrero, Z. Hekss and F. Giri, "Hybrid automaton-fuzzy control of single phase dual buck half bridge shunt active power filter for shoot through elimination and power quality improvement", International Journal of Electrical Power & Energy Systems, vol. 131, p. 106986, 2021.
[22] M. Badoni, A. Singh, S. Pandey and B. Singh, "Fractional Order Notch Filter for Grid-Connected Solar PV System with Power Quality Improvement", IEEE Transactions on Industrial Electronics, pp. 1-1, 2021.

[23] N. Babu P, J. Guerrero, P. Siano, R. Peesapati and G. Panda, "An Improved Adaptive Control Strategy in Grid-Tied PV System With Active Power Filter for Power Quality Enhancement", IEEE Systems Journal, vol. 15, no. 2, pp. 2859-2870, 2021.
[24] A. Mishra, S. Das, P. Ray, R. Mallick, A. Mohanty and D. Mishra, "PSO-GWO Optimized Fractional Order PID Based Hybrid Shunt Active Power Filter for Power Quality Improvements", IEEE Access, vol. 8, pp. 74497-74512, 2020.
[25] I. Melo, J. Pereira, A. Variz and P. Ribeiro, "Allocation and sizing of single tuned passive filters in three-phase distribution systems for power quality improvement", Electric Power Systems Research, vol. 180, p. 106128, 2020.
[26] G. Goswami and P. Goswami, "Power quality improvement at nonlinear loads using transformer-less shunt active power filter with adaptive neural fuzzy interface system supervised PID controllers", International Transactions on Electrical Energy Systems, vol. 30, no. 7, 2020.
[27] S. Prince, K. Panda and G. Panda, "Kalman filter variant intelligent control for power quality improvement in photovoltaic active power filter system", International Transactions on Electrical Energy Systems, vol. 30, no. 3, 2019.
[28] H. Shayeghi and Y. Hashemi, "Application of fuzzy decision-making based on INSGA-II to designing PV–wind hybrid system", Engineering Applications of Artificial Intelligence, vol. 45, pp. 1-17, 2015.
[29] S. Sudha Letha, T. Thakur and J. Kumar, "Harmonic elimination of a photo-voltaic based cascaded H-bridge multilevel inverter using PSO (particle swarm optimization) for induction motor drive", Energy, vol. 107, pp. 335-346, 2016.
[30] E. Jamil, S. Hameed, B. Jamil and Qurratulain, "Power quality improvement of distribution system with photovoltaic and permanent magnet synchronous generator based renewable energy farm using static synchronous compensator", Sustainable Energy Technologies and Assessments, vol. 35, pp. 98-116, 2019.
[31] M. Meral and D. Celik, "DSOGI-PLL Based Power Control Method to Mitigate Control Errors Under Disturbances of Grid Connected Hybrid Renewable Power Systems", Advances in Electrical and Electronic Engineering, vol. 16, no. 1, 2018.
[32] J. Arkhangelski, P. Roncero-Sánchez, M. Abdou-Tankari, J. Vázquez and G. Lefebvre, "Control and Restrictions of a Hybrid Renewable Energy System Connected to the Grid: A Battery and Supercapacitor Storage Case", Energies, vol. 12, no. 14, p. 2776, 2019.
[33] M.Naresh, U. K. Soni and R. K. Tripathi, "Power Flow Control and Power Quality Improvement in DFIG Based Wind Energy Conversion System Using Neuro Fuzzy System", International Journal of Applied Engineering Research, vol. 13, no.7, pp. 5236-5243, 2018.
[34] R. Muthukumar and P. Balamurugan, "A model predictive controller for improvement in power quality from a hybrid renewable energy system", Soft Computing, vol. 23, no. 8, pp. 2627-2635, 2018.
[35] R. Agarwal, I. Hussain and B. Singh, "LMF-Based Control Algorithm for Single Stage Three-Phase Grid Integrated Solar PV System", IEEE Transactions on Sustainable Energy, vol. 7, no. 4, pp. 1379-1387, 2016.
[36] K. Rathi and N. Prabha, "Grid Interconnected Photo Voltaic System Using Shunt Active Filter for Power Quality Improvement", International Journal of Power Electronics and Drive Systems (IJPEDS), vol. 9, no. 1, p. 365, 2018.
[37] Ghasemian, Hadi, FahimehGhasemian, and HamedVahdat-Nejad. "Human urbanization algorithm: A novel metaheuristic approach." Mathematics and Computers in Simulation, 2020.
[38] T. Le-Duc, Q. Nguyen and H. Nguyen-Xuan, "Balancing composite motion optimization", Information Sciences, vol. 520, pp. 250-270, 2020.
[39] H. Thanh Duong, H. Chi Phan, T. Le and N. Duc Bui, "Optimization design of rectangular concrete-filled steel tube short columns with Balancing Composite Motion Optimization and data-driven model", Structures, vol. 28, pp. 757-765, 2020.
[40] T. Nguyen, "A Data-Driven Assessment Based on Viscosity Resistance Coefficient Indicator of Bridge Spans Using Deep Learning and Balancing Composite Motion Optimization", Journal of Vibration Engineering & Technologies, 2021.